CD4+ T cell effector commitment coupled to self-renewal by asymmetric cell divisions

Simone A. Nish,[1,2] Kyra D. Zens,[3,4,5] Radomir Kratchmarov,[1,2] Wen-Hsuan W. Lin,[1,2] William C. Adams,[1,2] Yen-Hua Chen,[1,2] Bonnie Yen,[1,2] Nyanza J. Rothman,[1,2] Avinash Bhandoola,[6] Hai-Hui Xue,[7] Donna L. Farber,[3,4,5] and Steven L. Reiner[1,2]

[1]Department of Microbiology and Immunology and [2]Department of Pediatrics, College of Physicians and Surgeons, Columbia University, New York, NY 10032
[3]Columbia Center for Translational Immunology, [4]Department of Microbiology and Immunology, and [5]Department of Surgery, Columbia University Medical Center, New York, NY 10032
[6]T-Cell Biology and Development Unit, Laboratory of Genome Integrity, Center for Cancer Research, National Cancer Institute, Bethesda, MD 20892
[7]Department of Microbiology, Carver College of Medicine, University of Iowa, Iowa City, IA 52242

Upon infection, an activated CD4+ T cell produces terminally differentiated effector cells and renews itself for continued defense. In this study, we show that differentiation and self-renewal arise as opposing outcomes of sibling CD4+ T cells. After influenza challenge, antigen-specific cells underwent several divisions in draining lymph nodes (LN; DLNs) while maintaining expression of TCF1. After four or five divisions, some cells silenced, whereas some cells maintained TCF1 expression. TCF1-silenced cells were T helper 1–like effectors and concentrated in the lungs. Cells from earliest divisions were memory-like and concentrated in nondraining LN. TCF1-expressing cells from later divisions in the DLN could self-renew, clonally yielding a TCF1-silenced daughter cell as well as a sibling cell maintaining TCF1 expression. Some TCF1-expressing cells in DLNs acquired an alternative, follicular helper–like fate. Modeled differentiation experiments in vitro suggested that unequal PI3K/mechanistic target of rapamycin signaling drives intraclonal cell fate heterogeneity. Asymmetric division enables self-renewal to be coupled to production of differentiated CD4+ effector T cells during clonal selection.

The Journal of Experimental Medicine

INTRODUCTION

Upon infection, CD4+ T cells differentiate into short-lived effector cells as well as long-lived memory cells that mount responses upon re-exposure to the microbe. CD4+ T cells have the ability to differentiate into multiple effector subsets including T helper 1 cells (Th1 cells). The Th1 subset is defined by expression of the lineage-determining transcription factor T-bet and the capacity to secrete the effector molecule IFN-γ (Zhu et al., 2010). Th1 cells migrate to the site of microbial entry to exert their function (Swain et al., 2012). After the contraction phase, wherein the vast majority of effector cells undergo apoptosis, a small portion of cells persist in the host as memory T cells to combat future infections. Memory T cells can be divided into different subsets based on distinct effector function and homing capacity (Sallusto et al., 1999; Masopust et al., 2001; Reinhardt et al., 2001). One population of memory cells called central memory cells share similar features with naive T cells. They are characterized by expression of the chemokine receptor CCR7 and L-selectin (CD62L), circulate through secondary lymphoid organs, and have a less differentiated phenotype than bona fide effector cells. Upon rechallenge, they have the ability to regenerate differentiated effector cells in addition to self-renewing the central memory pool (Sallusto et al., 1999; Reinhardt et al., 2001; Zaph et al., 2004). In contrast, effector memory cells do not express CCR7 or CD62L and produce effector cytokines.

Using a variety of approaches, it has been suggested that a single T or B lymphocyte can generate progeny with intraclonal effector subclass diversity and memory cell renewal (Stemberger et al., 2007; Gerlach et al., 2010, 2013; Buchholz et al., 2013; Plumlee et al., 2013; Tubo et al., 2013, 2016; Graef et al., 2014; Becattini et al., 2015; Taylor et al., 2015). Whether cell-intrinsic, cell-extrinsic, stochastic, or deterministic mechanisms are responsible for the generation of intraclonal cell fate diversity of lymphocytes is an unresolved issue (Reiner and Adams, 2014). In this study, we have identified discrete stages of CD4+ T cell clonal selection distinguished by cell division, TCF1 expression, and anatomical localization. TCF1^{hi} cells had a less differentiated phenotype, showed increased expression of CD62L, and homed to noninflamed secondary lymphoid organs within the initial cell divisions. TCF1^{hi} cells from later divisions in the draining LNs (DLNs) had the capacity to asymmetrically self-renew while also generating PI3K-driven, TCF1^{lo} Th1 effector cells. The Th1 cell–like, TCF1^{lo} cells appeared incapable of reverting to central memory–phenotype cells and instead migrated to the site of infec-

Correspondence to Steven L. Reiner: sr2978@cumc.columbia.edu

Abbreviations used: CPD, cell proliferation dye; CTV, cell trace violet; DLN, draining LN; mTOR, mechanistic target of rapamycin; NDLN, nondraining LN; SLAM, signaling lymphocyte activation molecule; Tfh cell, T follicular helper cell.

The Rockefeller University Press $30.00
J. Exp. Med. 2017 Vol. 214 No. 1 39–47
https://doi.org/10.1084/jem.20161046

tion. Some of the TCF1^{hi} cells in the DLNs also appeared to be T follicular helper cell (Tfh cell)–like and noncirculating. These findings offer a potential mechanistic explanation for the seemingly hard-wired regeneration and functional diversity of CD4$^+$ T cell clonal selection (Tubo et al., 2013, 2016; Becattini et al., 2015).

RESULTS AND DISCUSSION

Early divergence of antigen-specific CD4$^+$ T cells distinguished by TCF1 expression, cell division, and anatomical location

TCF1 is a key regulator of T cell development in the thymus (Germar et al., 2011; Weber et al., 2011). In the periphery, TCF1 has been shown to be a negative regulator of effector cell and a positive regulator of memory cell CD8$^+$ responses (Jeannet et al., 2010; Zhao et al., 2010; Zhou et al., 2010; Thaventhiran et al., 2013; Tiemessen et al., 2014). To examine the expression of TCF1 in CD4$^+$ T cell responses, we used influenza viral infection, in which the primary activation of responding CD4$^+$ T cells (mediastinal LNs) is anatomically distinct from the site of Th1 effector function (lung tissue). OTII T cells were labeled with a cell proliferation dye (CPD) and adoptively transferred into Thy1 disparate recipient mice, which were subsequently infected intranasally with a recombinant strain of PR8 influenza virus expressing a peptide epitope of OVA recognized by the OTII TCR (hereafter referred to as PR8-OVA). TCF1 expression was examined in the dividing antigen-specific OTII T cells in the LNs draining the site of infection (mediastinal LNs and DLNs), the nondraining LNs (NDLNs), and the lungs on day 4 after infection (Fig. 1 A).

After approximately four to five divisions in the DLNs, a population of cells that had repressed TCF1 emerged alongside a population of cells that had retained TCF1 expression (Fig. 1 A). In contrast to DLNs, the lung, site of effector T cell function, and the NDLNs, site of central memory cell recirculation (Zaph et al., 2004; Colpitts and Scott, 2010), were each enriched in an exclusive subset (Fig. 1 A). Lungs were enriched for cells that had undergone greater division (five to seven rounds) and down-regulated TCF1, whereas NDLNs were enriched with cells that divided less (one to four divisions) and maintained high levels of TCF1.

Both TCF1^{hi} and TCF1^{lo} CD4$^+$ T cell subsets showed similar levels of CD44 induction, as well as CD127 (IL-7rα) and CCR7 repression (Fig. 1 B). In contrast, TCF1^{hi} cells had detectably less expression of the markers associated with Th1 cell differentiation, T-bet, CD25, and signaling lymphocyte activation molecule (SLAM; Fig. 1 B). Compared with TCF1^{lo} cells, lower Th1 cell–associated markers (despite comparable CD44 expression) were evident in TCF1^{hi} cells from both NDLNs and DLNs (Fig. 1 B) and across early and later TCF1^{hi} cell divisions (Fig. 1 C). Compared with the TCF1^{lo} subset, the TCF1^{hi} population also showed an increased percentage of cells that expressed CD62L (Fig. 1 D), which may explain the enrichment of TCF1^{hi} cells in lymphoid sites (Fig. 1 A).

In addition to central memory cells, other TCF1^{hi} progeny that reside in DLNs would include Tfh cells (Choi et al., 2015; Wu et al., 2015; Xu et al., 2015). We found a detectable portion of the TCF1^{hi} cells in the DLNs expressed substantial levels of the chemokine receptor CXCR5 and the transcription factor Bcl6, markers used to identify the Tfh cell lineage (Fig. 1 E). However, unlike the DLNs, the NDLNs and lung contained few if any Tfh-phenotype cells (Fig. 1 F). Within the first few days of infection, descendants of naive CD4$^+$ T cells appeared to exhibit regenerative and functional diversity that could be delineated by division, TCF1 expression, and anatomical localization.

Tcf7 expression marks CD4$^+$ T cells with the ability to self-renew

Among the later cell divisions in the DLNs, repression of TCF1 appears to mark Th1-like cells (with higher expression of CD25, SLAM, and T-bet) that are programmed to populate the site of infection. In contrast, TCF1^{hi} cells appear to be less differentiated and more likely to retain lymphoid homing capacity. We therefore wished to determine the flexibility and interrelatedness of the two populations. TCF1 is encoded by the *Tcf7* locus, and we therefore used OTII$^+$ *Tcf7*-GFP/+ reporter mice (Choi et al., 2015) to trace the fate of expressing and nonexpressing cells from PR8-OVA–infected recipient mice. We first determined that the pattern of *Tcf7*-GFP reporter expression in the DLNs (Fig. 2 A) was similar to TCF1 protein expression (Fig. 1 A), which established this reporter line as a suitable tool for investigating lineage relationships between *Tcf7*-GFP–high and *Tcf7*-GFP–low subsets.

We next sorted *Tcf7*-GFP–high and *Tcf7*-GFP–low OTII$^+$ CD4$^+$ T cells by flow cytometry from the DLNs of PR8-OVA–infected recipient mice. Equal numbers of sorted *Tcf7*-GFP–high and *Tcf7*-GFP–low cells were individually restimulated with anti-CD3 and anti-CD28 in vitro (Fig. 2 B). We found that the dividing *Tcf7*-GFP–high cells maintained the *Tcf7*-GFP–high pool while also abundantly giving rise to *Tcf7*-GFP–low cells (Fig. 2 B). However, the *Tcf7*-GFP–low cells simply generated more *Tcf7*-GFP–low cells (Fig. 2 B). To rule out the possibility that the difference in the ability to self-renew between the *Tcf7*-GFP–high and *Tcf7*-GFP–low cells was caused by a difference in the rounds of division they had undergone, we compared *Tcf7*-GFP–high and *Tcf7*-GFP–low cells that had divided the same number of times (five to eight rounds). After relabeling with division dye and restimulation, we found that the *Tcf7*-GFP–high cells divided further and self-renewed, producing more *Tcf7*-GFP–high and making *Tcf7*-GFP–low progeny. *Tcf7*-GFP–low cells also divided more but only produced additional *Tcf7*-GFP–low progeny (Fig. 2 C).

We obtained similar results from a system of modeled effector differentiation. Stimulation of naive T cells in Th1 cell–inducing conditions in vitro recapitulated the TCF1 protein expression heterogeneity in the progeny of activated CD4$^+$ T cells. Naive CD4$^+$ T cells were purified and stimu-

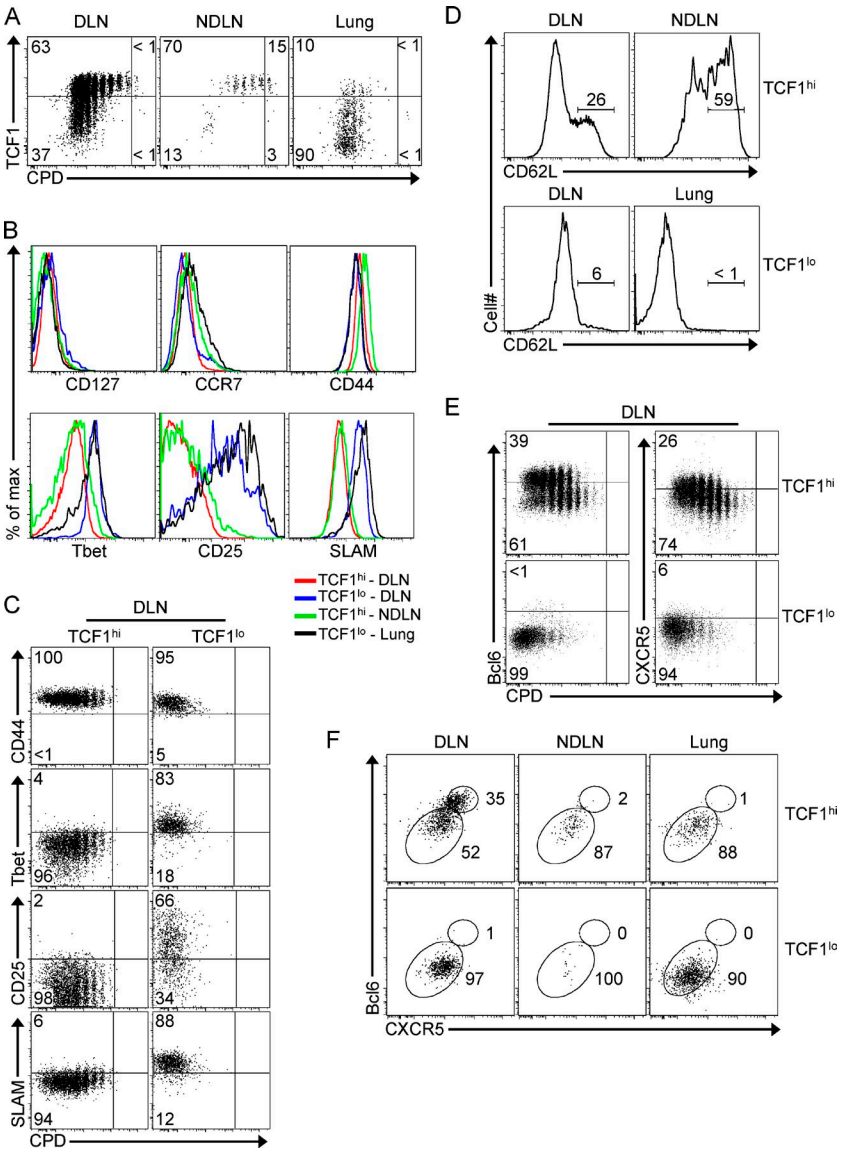

Figure 1. **Early divergence of antigen-specific CD4$^+$ T cells distinguished by TCF1 expression, cell division, and anatomical location.** (A) Purified OTII$^+$ CD4$^+$ T cells were labeled with a CPD and transferred into congenically disparate mice that were infected with PR8-OVA influenza virus. CPD versus TCF1 protein expression of donor cells was examined in the indicated organs 4 d after infection. Data are representative of eight independent experiments in which each sample represented a pool of cells from four infected mice. Significance of the mean percentage ± SEM for TCF1^{hi} versus TCF1^{lo} in DLN, $P < 0.0001$; TCF1^{hi} versus TCF1^{lo} in NDLN, $P < 0.0001$; TCF1^{hi} versus TCF1^{lo} in lungs, $P < 0.0001$; TCF1^{hi} in DLNs versus NDLNs, NS; TCF1^{lo} in DLNs versus NDLNs, $P = 0.0186$; TCF1^{hi} in NDLNs versus lungs, $P = 0.0001$; TCF1^{lo} in NDLNs versus lungs, $P = 0.0001$; TCF1^{hi} in DLNs versus lungs, $P = 0.0001$; TCF1^{lo} in DLNs versus lungs, $P = 0.0001$. (B) Expression of the indicated markers in OTII$^+$ TCF1^{hi} and TCF1^{lo} cells from the indicated organs on day 4 after infection. (C) CPD versus the indicated markers in TCF1^{hi} and TCF1^{lo} cells from the mediastinal DLNs on day 4 after infection. Significance of the mean percentage ± SEM of CD44$^+$ in TCF1^{hi} versus TCF1^{lo}, NS; Tbet$^+$ in TCF1^{hi} versus TCF1^{lo}, $P = 0.0044$; CD25$^+$ in TCF1^{hi} versus TCF1^{lo}, $P = 0.0013$. The mean percentage ± SEM of SLAM$^+$ in TCF1^{hi} and TCF1^{lo} was 6.78 ± 0.94 and 77.35 ± 16.75, respectively. Data are representative of two or more independent experiments, in which each sample represented a pool of cells from four infected mice. (D) CD62L expression in OTII$^+$ TCF1^{hi} and TCF1^{lo} cells from the indicated organs 5 d after infection. The mean percentage ± SEM of CD62L$^+$ in TCF1^{hi} and TCF1^{lo} in DLNs was 26.1 ± 0.1 and 5.99 ± 0.01, respectively; CD62L$^+$ cells in TCF1^{hi} in NDLNs was 55.6 ± 3.4; CD62L$^+$ in TCF1^{lo} in lungs was 0.765 ± 0.015. Data are representative of two independent experiments, in which each sample represented a pool of cells from four infected mice. (E) CPD, Bcl6, and CXCR5 expression in TCF1^{hi} and TCF1^{lo} OTII$^+$ cells in the DLNs on day 4 after infection. Significance of the mean percentage ± SEM of Bcl6$^+$ in TCF1^{hi} versus TCF1^{lo} in the DLNs, $P < 0.0094$. Data are representative of three independent experiments in which each sample represented a pool of cells from four infected mice. (F) Expression of CXCR5 and Bcl6 in TCF1^{hi} and TCF1^{lo} cells from the indicated organs on day 4 after infection. Significance of the mean percentage ± SEM of Bcl6$^+$ cells in TCF1^{hi} in DLNs versus NDLNs, $P < 0.0013$; Bcl6$^+$ in TCF1^{hi} in DLNs versus lungs, $P < 0.0014$; Bcl6$^+$ in TCF1^{hi} versus TCF1^{lo} in DLNs, $P < 0.0005$. Data are representative of four independent experiments, in which each sample represented a pool of cells from four infected mice. P-values were calculated using a two-tailed Student's *t* test.

lated in vitro with plate-bound anti-CD3 and anti-CD28 in the presence of IL-2 and IL-12 and were analyzed on days 3–6 of culture for TCF1 protein expression (Fig. 3 A). After about four cell divisions, a population of cells that showed low TCF1 protein abundance emerged, whereas some cells remained high for TCF1 protein content. Similarly, CD4$^+$ *Tcf7*-GFP T cells stimulated in Th1 cell–inducing conditions for 5 d also exhibited heterogeneity of GFP expression after a few cell divisions (Fig. 3 B). Then, we sorted the *Tcf7*-GFP–high and *Tcf7*-GFP–low cells, relabeled them with division dye, and restimulated them with plate-bound anti-CD3 and anti-CD28 for an additional 5 d. Similar to observations with ex vivo cells, we found that in vitro–derived *Tcf7*-GFP–high cells remained bipotent, able to generate *Tcf7*-GFP–low and *Tcf7*-GFP–high cells, whereas *Tcf7*-GFP–low cells were unable to revert to production of *Tcf7*-GFP–high cells (Fig. 3 C).

We also cultured *Tcf7*-GFP/+ cells in Th1 cell–inducing conditions for a longer period of time, 7 d, which allowed the *Tcf7*-GFP–high cells to undergo more rounds of division (Fig. 3 D). *Tcf7*-GFP–high and *Tcf7*-GFP–low

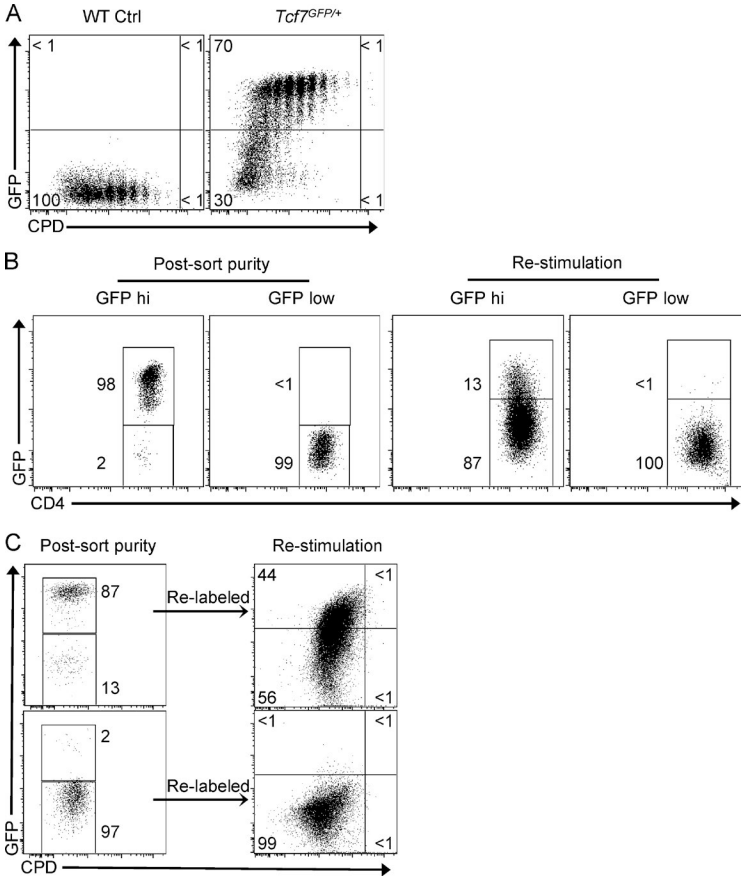

Figure 2. ***Tcf7*expression marking CD4$^+$ T cells capable of differentiation and self-renewal in vivo.** (A) Purified OTII$^+$ wild-type or OTII$^+$ *Tcf7*-GFP/+ CD4$^+$ T cells were labeled with CPD and transferred into recipient mice, which were subsequently infected with PR8-OVA influenza virus. CPD versus *Tcf7*-GFP expression was assessed in cells from the mediastinal LNs on day 5 after infection. Ctrl, control. (B, left) *Tcf7*-GFP–high and –low cells were purified by flow cytometry 5 d after infection. (Right) *Tcf7*-GFP expression after 5-d restimulation of the indicated sorted populations using plate-bound anti-CD3 and anti-CD28. GFP-high–sorted population: mean percentage ± SEM of GFP-high cells after restimulation was 10.97 ± 1.735 and of GFP-low cells was 88.8 ± 1.6. GFP-low–sorted population: mean percentage ± SEM of GFP-high cells after restimulation was 0.72 ± 0.49 and of GFP-low cells was 99 ± 0.7. Data are representative of two independent experiments, in which each sample represented a pool of cells from four to seven infected mice. (C) *Tcf7*-GFP–high and –low cells that had undergone five to eight divisions were sorted by flow cytometry from PR8-OVA–infected mice on day 5 after infection, relabeled with CPD, and restimulated with anti-CD3 and anti-CD28 for 5 d. GFP-high–sorted population: mean percentage ± SEM of GFP-high cells remaining after restimulation was 37.7 ± 6.3 and of GFP-low cells was 62.25 ± 6.25. GFP-low–sorted population: mean percentage ± SEM of GFP-high cells after restimulation was 1.375 ± 0.975 and of GFP-low cells was 98.3 ± 0.8. Data are representative of two independent experiments, in which each sample represented a pool of cells from four to seven infected mice.

cells from matched later divisions were sorted by flow cytometry, relabeled with CPD, and restimulated with anti-CD3 and anti-CD28 for 5 d. *Tcf7*-GFP–high cells divided further and remained bipotent, able to generate *Tcf7*-GFP–low and *Tcf7*-GFP–high cells, whereas *Tcf7*-GFP–low cells divided further but were unable to revert to production of *Tcf7*-GFP–high cells (Fig. 3 D). Therefore, *Tcf7* expression appears to mark a subset of CD4$^+$ T cells with the ability to self-renew. Silencing of *Tcf7* during commitment to effector differentiation, in contrast, appears to mark the inability to revert to a state of self-renewal.

PI3K signals drive mechanistic target of rapamycin (mTOR) activation, TCF1 silencing, and Th1 cell differentiation

It has been suggested that IL-2 drives the down-regulation of TCF1 in CD4$^+$ T cells (Wu et al., 2015). We found that activating CD4$^+$ T cells with plate-bound anti-CD3 and anti-CD28 in the presence of IL-2 or IL-12 repressed TCF1 expression (Fig. 4 A). PI3K signaling is important for driving repression of TCF1 in CD8$^+$ T cells and Pax5 in B cells (Lin et al., 2015). The effect of the cytokines on TCF1 repression in CD4$^+$ T cells was indeed PI3K dependent insofar as addition of the small molecule inhibitor of PI3K, LY294002, reversed the repression of TCF1 (Fig. 4, A and B). Cells that were generated in the presence of the PI3K inhibitor also underwent fewer rounds of division, failed to produce IFN-γ, granzyme B, and TNF, and were unable to induce expression of Blimp-1, which is known to promote terminal differentiation (Fig. 4, B and C). We also noted that activated CD4$^+$ T cells were heterogeneous for the activation of mTOR, as assessed by phospho-S6 ribosomal protein (Fig. 4 D). The subpopulation with high mTOR activity appeared to be the cells undergoing TCF1 silencing and terminal maturation insofar as PI3K inhibitor treatment coordinately suppressed the generation of each of those attributes. These results demonstrate that PI3K signaling is also critical for the activation of mTOR, repression of TCF1, and effector commitment in CD4$^+$ T cells.

Asymmetric TCF1 expression in dividing sibling CD4$^+$ T cells

How heterogeneity is generated in the CD4$^+$ T cell compartment is poorly understood. The PI3K-dependent bimodality in expression of TCF1 (Fig. 4 B) prompted us to test whether unequal signaling to TCF1 repression could bifurcate CD4$^+$ T cell fates. OTII$^+$ CD4$^+$ T cells sorted from recipient mice 4 d after PR8-OVA infection were examined for expression of TCF1 by confocal microscopy. TCF1 was localized to the nucleus in interphase cells. In metaphase cells, TCF1 was excluded from condensed chromatin and symmetrically localized to the cytoplasm. In contrast to the invariant symmetry of TCF1 in metaphase, ∼74% of conjoined sibling pairs, iden-

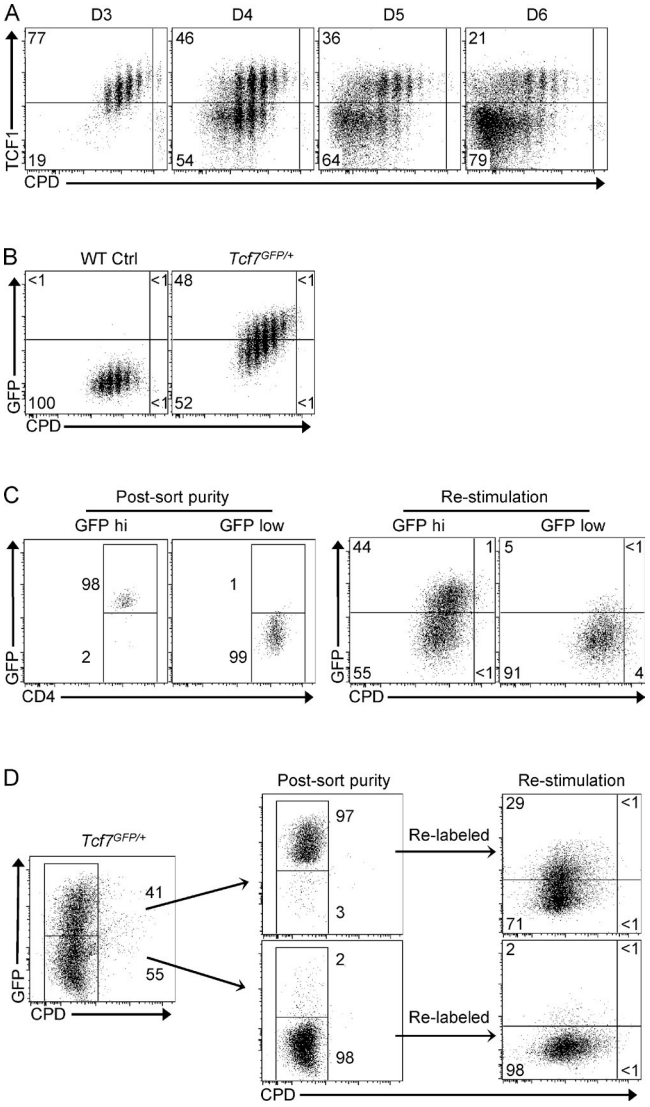

Figure 3. **Expression of *Tcf7* marking in vitro–derived CD4$^+$ T cells capable of self-renewal.** (A) CPD versus TCF1 protein expression of naive CD4$^+$ T cells stimulated with plate-bound anti-CD3 and anti-CD28 plus recombinant IL-2 and IL-12 (Th1 cell–inducing conditions) for the indicated times. Data are representative of two independent experiments. (B) CPD versus *Tcf7*-GFP expression of naive, wild-type, or *Tcf7*-GFP/+ CD4$^+$ T cells stimulated for 5 d in vitro with plate-bound anti-CD3 and anti-CD28 plus recombinant IL-2 and IL-12. Ctrl, control. (C) Sorted, *Tcf7*-GFP–high and *Tcf7*-GFP–low CD4$^+$ T cells 5 d after stimulation under Th1 cell–inducing conditions were relabeled with CPD, restimulated for an additional 5 d with plate-bound anti-CD3 and anti-CD28, and assessed for CPD versus *Tcf7*-GFP expression. GFP-high–sorted population: mean percentage ± SEM of GFP-high cells after restimulation was 35.3 ± 8.1 and of GFP-low cells was 63.6 ± 8.4. GFP-low–sorted population: mean percentage ± SEM of GFP-high cells after restimulation was 5.6 ± 1 and of GFP-low cells was 90.5 ± 0.4. Data are representative of two independent experiments. (D) *Tcf7*-GFP reporter CD4$^+$ T cells stimulated in Th1 cell–inducing conditions for 7 d were sorted, relabeled with CPD, restimulated for an additional 5 d with anti-CD3 and anti-CD28, and assessed for CPD versus *Tcf7*-GFP expression. GFP-high–sorted population: mean percentage ± SEM of GFP-high cells remaining after restimulation was 23.35 ± 5.65 and of GFP-low cells was 75.9 ± 5. GFP-low–sorted population: mean percentage ± SEM of GFP-high cells after restimulation was 4.6 ± 2.445 and of GFP-low cells was 94.7 ± 2.8. Data are representative of two independent experiments.

tified by the presence of an intercellular cytoplasmic bridge containing tubulin, contained asymmetric abundance of TCF1 (Fig. 5, A and B). Similar results were obtained from in vitro differentiation, with 56% of cytokinetic sibling pairs having asymmetric TCF1 abundance (Fig. 5, C and D). The asymmetric expression of TCF1 in cytokinetic cells does not appear to be caused by unequal partitioning of preformed TCF1 protein during metaphase but rather a signaling event occurring after telophase, which is consistent with recent findings in B cells and CD8$^+$ T cells (Lin et al., 2015).

Our findings suggest that maintenance of expression of TCF1 among the progeny of a selected CD4$^+$ T cell marks a subset of cells that have undergone few divisions and retained capacity for lymphoid recirculation, resembling canonical central memory cells. TCF1 expression also marks cells that have divided more, remained in the DLNs, and are capable of producing TCF1^{lo}, Th1 effector progeny, also renewing the TCF1^{hi} fate during active infection. Whether those TCF1^{hi} cells that are producing Th1 cell progeny and self-renewing during antigen encounter will die or, instead, revert to quiescence after resolution of infection will require further investigation. In contrast to the bipotency of TCF1^{hi} cells, TCF1 repression in Th1 cells appears to mark an inability to revert to the TCF1^{hi} fate under the physiological conditions tested here.

Among the TCF1^{hi} cells in the DLNs, we also found a subset of cells with Tfh cell characteristics, consistent with other recent studies revealing a role for TCF1 in Tfh cell development (Choi et al., 2015; Wu et al., 2015; Xu et al., 2015). Insofar as Tfh cells possess characteristics of memory-like renewal (Choi et al., 2013; Hale et al., 2013; Suan et al., 2015), it is notable that self-renewing CD4$^+$ and CD8$^+$ T cells can share phenotypic markers with Tfh cells, such as expression of CXCR5 (Pepper et al., 2011; He et al., 2016; Im et al., 2016; Leong et al., 2016; Utzschneider et al., 2016). The present findings suggest that TCF1^{hi} cell self-renewal occurs in the daughter cells with weaker anabolic (PI3K/mTOR) signaling, whereas TCF1^{lo} Th1 effector cells emerge from the daughter cells with stronger PI3K/mTOR signaling. Tfh cells also appear to diverge from Th1 cells owing to a weaker versus stronger PI3K/AKT/mTOR signaling divergence (Ray et al., 2015; Wu et al., 2015). The nature and extent of the phenotypic, functional, and metabolic similarities between central memory and Tfh cells, as well as the corresponding differences between those two subsets and Th1 cells, will also require further investigation.

An enigmatic finding in the current study, which is analogous to recent observations of TCF1 and Pax5 heterogeneity in CD8$^+$ T cells and B cells, respectively (Lin et al., 2015), is why there exists a lag of three or four divisions

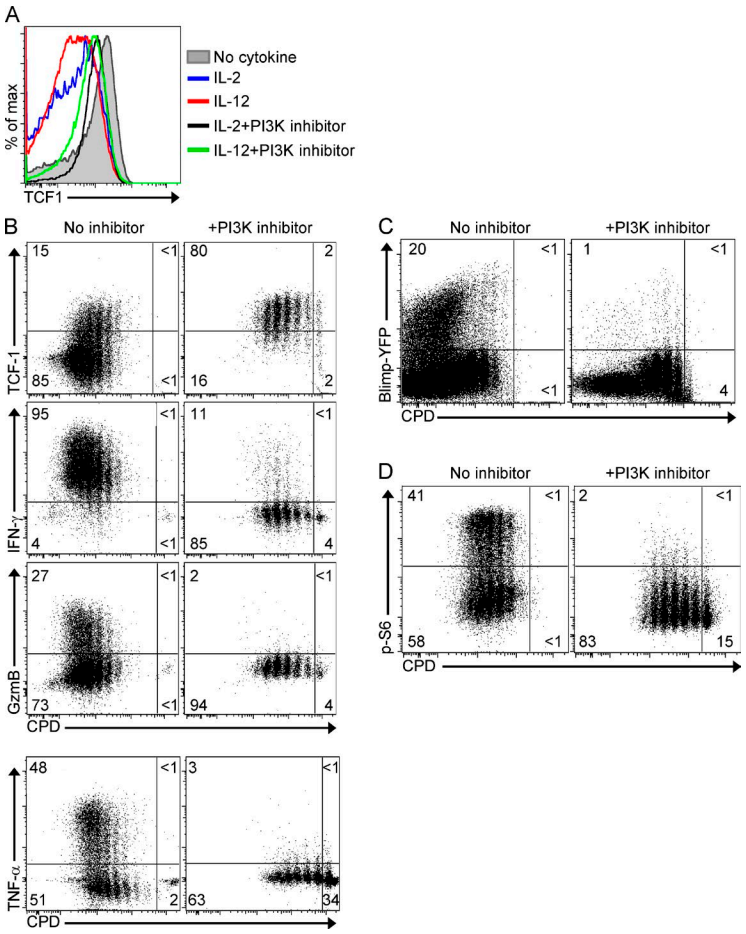

Figure 4. **PI3K signaling driving TCF1 repression and Th1 effector differentiation in CD4⁺ T cells.** (A) TCF1 protein expression in CD4⁺ T cells stimulated for 5 d with plate-bound anti-CD3 and anti-CD28 in the absence or presence of IL-2 or IL-12, without or with 5 µM PI3K inhibitor. (B) CPD versus TCF1, granzyme B (GzmB), IFN-γ, and TNF-α in CD4⁺ T cells stimulated for 5 d in Th1 cell–inducing conditions (IL-2 and IL-12) in the absence or presence of PI3K inhibitor. TNF expression was analyzed in separate experiments from granzyme B and IFN-γ. Significance of the mean percentage ± SEM of TCF1^{hi} in the absence versus presence of inhibitor, $P < 0.0001$; IFN-γ⁺ in the absence versus presence of inhibitor, $P = 0.0022$. The mean percentage ± SEM of granzyme B⁺ in the absence and presence of inhibitor was 24.5 ± 2.5 and 1.07 ± 0.82, respectively. TNF⁺ in the absence and presence of inhibitor was 45.15 ± 2.35 and 6.735 ± 4.365, respectively. Data are representative of two or more independent experiments. (C) CPD versus Blimp-1–YFP expression in CD4⁺ T cells stimulated for 6 d in Th1 cell–inducing conditions in the absence or presence of PI3K inhibitor. Significance of the mean percentage ± SEM of Blimp-1–YFP⁺ cells in the absence versus presence of inhibitor, $P = 0.0357$. Data are representative of three independent experiments. (D) CPD versus phospho-S6 (p-S6) in CD4⁺ T cells stimulated for 5 d in Th1 cell–inducing conditions in the absence or presence of PI3K inhibitor. Significance of the mean percentage ± SEM of phospho-S6⁺ cells in the absence versus presence of PI3K inhibitor, $P = 0.0074$. Data are representative of three independent experiments. P-values were calculated using a two-tailed Student's *t* test.

before silencing TCF1 expression. In CD4⁺ T cells undergoing Th2 cell differentiation, there is an analogous lag in induction of IL-4 expression (Bird et al., 1998). Insofar as strong but unequal PI3K/mTOR signaling appears to commence from the very first T cell divisions (Lin et al., 2015; Pollizzi et al., 2016; Verbist et al., 2016), there would seem to exist some other rate-limiting feature, resolved by cell division, that delays gene silencing or induction. In B and T cells, silencing of genes associated with terminal differentiation appears to result from de novo establishment of epigenetic silencing, which may require more than one cell division (Scharer et al., 2013; Caron et al., 2015; Barwick et al., 2016; Ladle et al., 2016). Synthesis of the posttranslational modifications (such as acetyl and methyl groups) that induce or silence gene activity may also require some time- or division-dependent metabolic remodeling (Lu and Thompson, 2012; Londoño Gentile et al., 2013). Future studies examining signaling, epigenetic, and metabolic changes during the first three cell divisions may help resolve the nature of this division-linked lag in differentiation. In summary, the present findings suggest that metabolic inequality during cell division might ensure determinism for memory cell self-renewal as well as diversification of effector subclasses during the clonal selection of a CD4⁺ T cell.

MATERIALS AND METHODS

Mice

C57BL/6 mice and C57BL/6 OTII mice (with transgenic expression of an I-A^b–restricted TCR specific for OVA amino acids 323–339) were either bred at Columbia University or purchased from The Jackson Laboratory. C57BL/6 Blimp-1–YFP mice (Fooksman et al., 2010) and C57BL/6 *Tcf7*-GFP/+ mice (Choi et al., 2015) were previously described. Both male and female mice were used in the study. Mice were housed in specific pathogen–free conditions. All animal studies were performed according to the Institutional Animal Care and Use Guidelines of Columbia University.

Adoptive transfer and influenza virus infections

OTII wild-type CD4⁺ T cells were purified by magnetic cell separation (Miltenyi Biotec) and labeled with cell trace violet (CTV) proliferation dye. A total of 10^6 cells were adoptively transferred by intravenous injection into Thy1 disparate C57BL/6 recipient mice. The next day, mice were anesthetized by isoflurane and inoculated intranasally with 250 50% tissue culture infective doses of PR8-OVA influenza virus. Expression of different markers was examined on day 4 or 5 after infection. In some experiments, a total of 10^6 OTII Tcf7-GFP/+ CD4⁺ T cells were adoptively transferred into

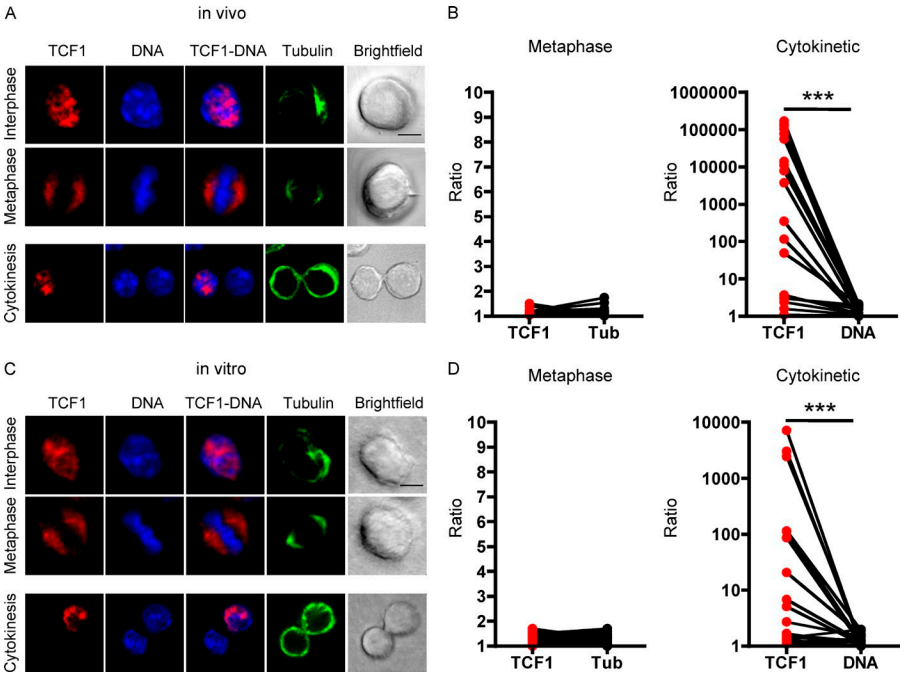

Figure 5. **Asymmetric TCF1 abundance in conjoined CD4⁺ T cell sibling pairs.** (A) Confocal image analysis of TCF1 protein staining in representative interphase, metaphase, and cytokinetic OTII⁺ CD4⁺ T cells 4 d after influenza infection. Cells were stained for TCF1 (red), DNA (blue), and α-tubulin (green). Bar, 4 µm. (B, left) The graph depicts ratio of TCF1 fluorescence between two sides of metaphase cells and ratio of tubulin (Tub). (Right) The graph depicts ratio of TCF1 fluorescence between sibling cells of a pair and ratio of DNA. Asymmetric TCF1 expression was observed in 74% of conjoined siblings. n = 19 sibling pairs. ***, P < 0.0001. Data are representative of three independent experiments, in which each sample represented a pool of cells from four infected mice. (C) Confocal image analysis of TCF1 protein staining in representative interphase, metaphase, and cytokinetic CD4⁺ T cells 3 d after Th1 cell–inducing conditions. Bar, 4 µm (D, left) The graph depicts ratio of TCF1 fluorescence between two sides of metaphase cells and ratio of tubulin. (Right) The graph depicts ratio of TCF1 fluorescence between sibling cells of a pair and ratio of DNA. Asymmetric TCF1 expression was observed in 56% of conjoined siblings. n = 18 sibling pairs. ***, P = 0.0003. Two-tailed Fisher's exact test was used to calculate p-values. Data are representative of two independent experiments.

recipient mice that were subsequently infected with PR8-OVA. *Tcf7*-GFP/+–high and –low cells were sorted on day 5 after infection, relabeled with a CPD (either CTV or eFluor 670), and restimulated to examine responses.

Cell culture

Naive WT CD4⁺ T cells purified by magnetic cell separation were labeled with CTV, and 5 × 10^5 cells were cultured in 48-well tissue culture plates that were precoated with 1 µg/ml anti-CD3 and anti-CD28 in the presence of 25 U/ml IL-2 and/or 10 ng/ml IL-12. In some experiments, a small molecule inhibitor to PI3K (5 µM), LY294002 (Cell Signaling Technology), was included at the start of the culture. Cells were harvested at the indicated time points. *Tcf7*-GFP/+–high and –low cells were also sorted, relabeled with CTV or eFluor 670 CPD, restimulated, and examined for expression of GFP.

Flow cytometry

Single-cell suspensions were prepared, and cells were stained according to standard staining protocol. Surface staining was done with the following antibodies: CD4 (RM4-5; BD), CD127 (A7R34; eBioscience), CCR7 (4B12; eBioscience), CD44 (IM7; BioLegend), SLAM (TC15-12F12.2; BioLegend), CD62L (MEL-14; BD), CXCR5 (2G8; BD), and CD25 (PC61; BD). Intracellular staining was done with the following antibodies: T-bet (4B10; BioLegend), TCF1 (C63D9; Cell Signaling Technology), Bcl6 (K112-91; BD), and phospho-S6 (S235/236; Cell Signaling Technology). Flow cytometry was acquired on LSRII and Fortessa machines (BD), and analysis was performed with FlowJo software (Tree Star).

Confocal microscopy

Immunofluorescence was performed as previously described (Chang et al., 2007; Barnett et al., 2012; Ciocca et al., 2012; Lin et al., 2015). In brief, FACS-purified cells were transferred to poly-L-lysine–coated coverslips (no. 1.5) and incubated at 37°C for adherence. Cells were fixed with 3% paraformaldehyde, and after rehydration in 50 mM NH_4Cl in PBS, cells were permeabilized with 0.3% Triton X-100 in PBS and then incubated in blocking buffer (0.01% saponin and 0.25% fish skin gelatin in PBS). Cells were stained with primary and secondary antibodies diluted in blocking buffer. Images were acquired on a laser-scanning inverted confocal microscope (LSM710; ZEISS), and total fluorescence in cells was quantified using ImageJ software (National Institutes of Health). The following primary antibodies were used: rat anti–α-tubulin (YOL1/34; Abcam) and rabbit anti-TCF1 (C63D9; Cell Signaling Technology). The following secondary antibodies were used: goat α-rat AF488 and goat α-rabbit AF568. ProlongGold with DAPI (Invitrogen) was used to

stain DNA and mount coverslips on glass slides. TCF1 protein was considered asymmetric in conjoined cells if the ratio of the fluorescence was greater than the mean of DNA plus two standard deviations. P-values were calculated with two-tailed Fisher's exact test.

ACKNOWLEDGMENTS

This study was supported by National Institutes of Health grants (AI061699, AI113365, and AI076458 to S.L. Reiner and AI112579, AI115149, AI119160, and AI121080 to H.-H. Xue) and the U.S. Department of Veterans Affairs Merit Review Award (I01 BX002903 to H.-H. Xue).

The authors declare no competing financial interests.

Author contributions: S.A. Nish and S.L. Reiner conceived and designed the study. S.A. Nish, R. Kratchmarov, K.D. Zens, W.-H.W. Lin, W.C. Adams, Y.-H. Chen, and B. Yen performed experiments. S.A. Nish and S.L. Reiner analyzed data and wrote the manuscript. N.J. Rothman assisted with animal experiments. A. Bhandoola and H.-H. Xue provided reagents and expertise.

Submitted: 6 July 2016
Revised: 6 October 2016
Accepted: 10 November 2016

REFERENCES

Barnett, B.E., M.L. Ciocca, R. Goenka, L.G. Barnett, J. Wu, T.M. Laufer, J.K. Burkhardt, M.P. Cancro, and S.L. Reiner. 2012. Asymmetric B cell division in the germinal center reaction. *Science.* 335:342–344. http://dx.doi.org/10.1126/science.1213495

Barwick, B.G., C.D. Scharer, A.P. Bally, and J.M. Boss. 2016. Plasma cell differentiation is coupled to division-dependent DNA hypomethylation and gene regulation. *Nat. Immunol.* 17:1216–1225. http://dx.doi.org/10.1038/ni.3519

Becattini, S., D. Latorre, F. Mele, M. Foglierini, C. De Gregorio, A. Cassotta, B. Fernandez, S. Kelderman, T.N. Schumacher, D. Corti, et al. 2015. Functional heterogeneity of human memory $CD4^+$ T cell clones primed by pathogens or vaccines. *Science.* 347:400–406. http://dx.doi.org/10.1126/science.1260668

Bird, J.J., D.R. Brown, A.C. Mullen, N.H. Moskowitz, M.A. Mahowald, J.R. Sider, T.F. Gajewski, C.R. Wang, and S.L. Reiner. 1998. Helper T cell differentiation is controlled by the cell cycle. *Immunity.* 9:229–237. http://dx.doi.org/10.1016/S1074-7613(00)80605-6

Buchholz, V.R., M. Flossdorf, I. Hensel, L. Kretschmer, B. Weissbrich, P. Gräf, A. Verschoor, M. Schiemann, T. Höfer, and D.H. Busch. 2013. Disparate individual fates compose robust $CD8^+$ T cell immunity. *Science.* 340:630–635. http://dx.doi.org/10.1126/science.1235454

Caron, G., M. Hussein, M. Kulis, C. Delaloy, F. Chatonnet, A. Pignarre, S. Avner, M. Lemarié, E.A. Mahé, N. Verdaguer-Dot, et al. 2015. Cell-cycle-dependent reconfiguration of the DNA methylome during terminal differentiation of human B cells into plasma cells. *Cell Reports.* 13:1059–1071. http://dx.doi.org/10.1016/j.celrep.2015.09.051

Chang, J.T., V.R. Palanivel, I. Kinjyo, F. Schambach, A.M. Intlekofer, A. Banerjee, S.A. Longworth, K.E. Vinup, P. Mrass, J. Oliaro, et al. 2007. Asymmetric T lymphocyte division in the initiation of adaptive immune responses. *Science.* 315:1687–1691. http://dx.doi.org/10.1126/science.1139393

Choi, Y.S., J.A. Yang, I. Yusuf, R.J. Johnston, J. Greenbaum, B. Peters, and S. Crotty. 2013. Bcl6 expressing follicular helper CD4 T cells are fate committed early and have the capacity to form memory. *J. Immunol.* 190:4014–4026. http://dx.doi.org/10.4049/jimmunol.1202963

Choi, Y.S., J.A. Gullicksrud, S. Xing, Z. Zeng, Q. Shan, F. Li, P.E. Love, W. Peng, H.H. Xue, and S. Crotty. 2015. LEF-1 and TCF-1 orchestrate T_{FH} differentiation by regulating differentiation circuits upstream of the transcriptional repressor Bcl6. *Nat. Immunol.* 16:980–990. http://dx.doi.org/10.1038/ni.3226

Ciocca, M.L., B.E. Barnett, J.K. Burkhardt, J.T. Chang, and S.L. Reiner. 2012. Cutting edge: Asymmetric memory T cell division in response to rechallenge. *J. Immunol.* 188:4145–4148. http://dx.doi.org/10.4049/jimmunol.1200176

Colpitts, S.L., and P. Scott. 2010. The early generation of a heterogeneous $CD4^+$ T cell response to *Leishmania major*. *J. Immunol.* 185:2416–2423. http://dx.doi.org/10.4049/jimmunol.1000483

Fooksman, D.R., T.A. Schwickert, G.D. Victora, M.L. Dustin, M.C. Nussenzweig, and D. Skokos. 2010. Development and migration of plasma cells in the mouse lymph node. *Immunity.* 33:118–127. http://dx.doi.org/10.1016/j.immuni.2010.06.015

Gerlach, C., J.W. van Heijst, E. Swart, D. Sie, N. Armstrong, R.M. Kerkhoven, D. Zehn, M.J. Bevan, K. Schepers, and T.N. Schumacher. 2010. One naive T cell, multiple fates in $CD8^+$ T cell differentiation. *J. Exp. Med.* 207:1235–1246. http://dx.doi.org/10.1084/jem.20091175

Gerlach, C., J.C. Rohr, L. Perié, N. van Rooij, J.W. van Heijst, A. Velds, J. Urbanus, S.H. Naik, H. Jacobs, J.B. Beltman, et al. 2013. Heterogeneous differentiation patterns of individual $CD8^+$ T cells. *Science.* 340:635–639. http://dx.doi.org/10.1126/science.1235487

Germar, K., M. Dose, T. Konstantinou, J. Zhang, H. Wang, C. Lobry, K.L. Arnett, S.C. Blacklow, I. Aifantis, J.C. Aster, and F. Gounari. 2011. T-cell factor 1 is a gatekeeper for T-cell specification in response to Notch signaling. *Proc. Natl. Acad. Sci. USA.* 108:20060–20065. http://dx.doi.org/10.1073/pnas.1110230108

Graef, P., V.R. Buchholz, C. Stemberger, M. Flossdorf, L. Henkel, M. Schiemann, I. Drexler, T. Höfer, S.R. Riddell, and D.H. Busch. 2014. Serial transfer of single-cell-derived immunocompetence reveals stemness of $CD8^+$ central memory T cells. *Immunity.* 41:116–126. http://dx.doi.org/10.1016/j.immuni.2014.05.018

Hale, J.S., B. Youngblood, D.R. Latner, A.U. Mohammed, L. Ye, R.S. Akondy, T. Wu, S.S. Iyer, and R. Ahmed. 2013. Distinct memory $CD4^+$ T cells with commitment to T follicular helper- and T helper 1-cell lineages are generated after acute viral infection. *Immunity.* 38:805–817. http://dx.doi.org/10.1016/j.immuni.2013.02.020

He, R., S. Hou, C. Liu, A. Zhang, Q. Bai, M. Han, Y. Yang, G. Wei, T. Shen, X. Yang, et al. 2016. Follicular CXCR5-expressing $CD8^+$ T cells curtail chronic viral infection. *Nature.* 537:412–428. http://dx.doi.org/10.1038/nature19317

Im, S.J., M. Hashimoto, M.Y. Gerner, J. Lee, H.T. Kissick, M.C. Burger, Q. Shan, J.S. Hale, J. Lee, T.H. Nasti, et al. 2016. Defining $CD8^+$ T cells that provide the proliferative burst after PD-1 therapy. *Nature.* 537:417–421. http://dx.doi.org/10.1038/nature19330

Jeannet, G., C. Boudousquié, N. Gardiol, J. Kang, J. Huelsken, and W. Held. 2010. Essential role of the Wnt pathway effector Tcf-1 for the establishment of functional CD8 T cell memory. *Proc. Natl. Acad. Sci. USA.* 107:9777–9782. http://dx.doi.org/10.1073/pnas.0914127107

Ladle, B.H., K.P. Li, M.J. Phillips, A.B. Pucsek, A. Haile, J.D. Powell, E.M. Jaffee, D.A. Hildeman, and C.J. Gamper. 2016. De novo DNA methylation by DNA methyltransferase 3a controls early effector $CD8^+$ T-cell fate decisions following activation. *Proc. Natl. Acad. Sci. USA.* 113:10631–10636. http://dx.doi.org/10.1073/pnas.1524490113

Leong, Y.A., Y. Chen, H.S. Ong, D. Wu, K. Man, C. Deleage, M. Minnich, B.J. Meckiff, Y. Wei, Z. Hou, et al. 2016. $CXCR5^+$ follicular cytotoxic T cells control viral infection in B cell follicles. *Nat. Immunol.* 17:1187–1196. http://dx.doi.org/10.1038/ni.3543

Lin, W.H., W.C. Adams, S.A. Nish, Y.H. Chen, B. Yen, N.J. Rothman, R. Kratchmarov, T. Okada, U. Klein, and S.L. Reiner. 2015. Asymmetric PI3K signaling driving developmental and regenerative cell fate bifurcation. *Cell Reports.* 13:2203–2218. http://dx.doi.org/10.1016/j.celrep.2015.10.072

Londoño Gentile, T., C. Lu, P.M. Lodato, S. Tse, S.H. Olejniczak, E.S. Witze, C.B. Thompson, and K.E. Wellen. 2013. DNMT1 is regulated by ATP-citrate lyase and maintains methylation patterns during adipocyte differentiation. *Mol. Cell. Biol.* 33:3864–3878. http://dx.doi.org/10.1128/MCB.01495-12

Lu, C., and C.B. Thompson. 2012. Metabolic regulation of epigenetics. *Cell Metab.* 16:9–17. http://dx.doi.org/10.1016/j.cmet.2012.06.001

Masopust, D., V. Vezys, A.L. Marzo, and L. Lefrançois. 2001. Preferential localization of effector memory cells in nonlymphoid tissue. *Science.* 291:2413–2417. http://dx.doi.org/10.1126/science.1058867

Pepper, M., A.J. Pagán, B.Z. Igyártó, J.J. Taylor, and M.K. Jenkins. 2011. Opposing signals from the Bcl6 transcription factor and the interleukin-2 receptor generate T helper 1 central and effector memory cells. *Immunity.* 35:583–595. http://dx.doi.org/10.1016/j.immuni.2011.09.009

Plumlee, C.R., B.S. Sheridan, B.B. Cicek, and L. Lefrançois. 2013. Environmental cues dictate the fate of individual $CD8^+$ T cells responding to infection. *Immunity.* 39:347–356. http://dx.doi.org/10.1016/j.immuni.2013.07.014

Pollizzi, K.N., I.H. Sun, C.H. Patel, Y.C. Lo, M.H. Oh, A.T. Waickman, A.J. Tam, R.L. Blosser, J. Wen, G.M. Delgoffe, and J.D. Powell. 2016. Asymmetric inheritance of mTORC1 kinase activity during division dictates $CD8^+$ T cell differentiation. *Nat. Immunol.* 17:704–711. http://dx.doi.org/10.1038/ni.3438

Ray, J.P., M.M. Staron, J.A. Shyer, P.C. Ho, H.D. Marshall, S.M. Gray, B.J. Laidlaw, K. Araki, R. Ahmed, S.M. Kaech, and J. Craft. 2015. The interleukin-2-mTORc1 kinase axis defines the signaling, differentiation, and metabolism of T helper 1 and follicular B helper T cells. *Immunity.* 43:690–702. http://dx.doi.org/10.1016/j.immuni.2015.08.017

Reiner, S.L., and W.C. Adams. 2014. Lymphocyte fate specification as a deterministic but highly plastic process. *Nat. Rev. Immunol.* 14:699–704. http://dx.doi.org/10.1038/nri3734

Reinhardt, R.L., A. Khoruts, R. Merica, T. Zell, and M.K. Jenkins. 2001. Visualizing the generation of memory CD4 T cells in the whole body. *Nature.* 410:101–105. http://dx.doi.org/10.1038/35065111

Sallusto, F., D. Lenig, R. Förster, M. Lipp, and A. Lanzavecchia. 1999. Two subsets of memory T lymphocytes with distinct homing potentials and effector functions. *Nature.* 401:708–712. http://dx.doi.org/10.1038/44385

Scharer, C.D., B.G. Barwick, B.A. Youngblood, R. Ahmed, and J.M. Boss. 2013. Global DNA methylation remodeling accompanies CD8 T cell effector function. *J. Immunol.* 191:3419–3429. http://dx.doi.org/10.4049/jimmunol.1301395

Stemberger, C., K.M. Huster, M. Koffler, F. Anderl, M. Schiemann, H. Wagner, and D.H. Busch. 2007. A single naive $CD8^+$ T cell precursor can develop into diverse effector and memory subsets. *Immunity.* 27:985–997. http://dx.doi.org/10.1016/j.immuni.2007.10.012

Suan, D., A. Nguyen, I. Moran, K. Bourne, J.R. Hermes, M. Arshi, H.R. Hampton, M. Tomura, Y. Miwa, A.D. Kelleher, et al. 2015. T follicular helper cells have distinct modes of migration and molecular signatures in naive and memory immune responses. *Immunity.* 42:704–718. http://dx.doi.org/10.1016/j.immuni.2015.03.002

Swain, S.L., K.K. McKinstry, and T.M. Strutt. 2012. Expanding roles for $CD4^+$ T cells in immunity to viruses. *Nat. Rev. Immunol.* 12:136–148.

Taylor, J.J., K.A. Pape, H.R. Steach, and M.K. Jenkins. 2015. Apoptosis and antigen affinity limit effector cell differentiation of a single naïve B cell. *Science.* 347:784–787. http://dx.doi.org/10.1126/science.aaa1342

Thaventhiran, J.E., D.T. Fearon, and L. Gattinoni. 2013. Transcriptional regulation of effector and memory $CD8^+$ T cell fates. *Curr. Opin. Immunol.* 25:321–328. http://dx.doi.org/10.1016/j.coi.2013.05.010

Tiemessen, M.M., M.R. Baert, L. Kok, M.C. van Eggermond, P.J. van den Elsen, R. Arens, and F.J. Staal. 2014. T cell factor 1 represses $CD8^+$ effector T cell formation and function. *J. Immunol.* 193:5480–5487. http://dx.doi.org/10.4049/jimmunol.1303417

Tubo, N.J., A.J. Pagán, J.J. Taylor, R.W. Nelson, J.L. Linehan, J.M. Ertelt, E.S. Huseby, S.S. Way, and M.K. Jenkins. 2013. Single naive $CD4^+$ T cells from a diverse repertoire produce different effector cell types during infection. *Cell.* 153:785–796. http://dx.doi.org/10.1016/j.cell.2013.04.007

Tubo, N.J., B.T. Fife, A.J. Pagan, D.I. Kotov, M.F. Goldberg, and M.K. Jenkins. 2016. Most microbe-specific naïve $CD4^+$ T cells produce memory cells during infection. *Science.* 351:511–514. http://dx.doi.org/10.1126/science.aad0483

Utzschneider, D.T., M. Charmoy, V. Chennupati, L. Pousse, D.P. Ferreira, S. Calderon-Copete, M. Danilo, F. Alfei, M. Hofmann, D. Wieland, et al. 2016. T cell factor 1-expressing memory-like $CD8^+$ T cells sustain the immune response to chronic viral infections. *Immunity.* 45:415–427. http://dx.doi.org/10.1016/j.immuni.2016.07.021

Verbist, K.C., C.S. Guy, S. Milasta, S. Liedmann, M.M. Kamiński, R. Wang, and D.R. Green. 2016. Metabolic maintenance of cell asymmetry following division in activated T lymphocytes. *Nature.* 532:389–393. http://dx.doi.org/10.1038/nature17442

Weber, B.N., A.W. Chi, A. Chavez, Y. Yashiro-Ohtani, Q. Yang, O. Shestova, and A. Bhandoola. 2011. A critical role for TCF-1 in T-lineage specification and differentiation. *Nature.* 476:63–68. http://dx.doi.org/10.1038/nature10279

Wu, T., H.M. Shin, E.A. Moseman, Y. Ji, B. Huang, C. Harly, J.M. Sen, L.J. Berg, L. Gattinoni, D.B. McGavern, and P.L. Schwartzberg. 2015. TCF1 is required for the T follicular helper cell response to viral infection. *Cell Reports.* 12:2099–2110. http://dx.doi.org/10.1016/j.celrep.2015.08.049

Xu, L., Y. Cao, Z. Xie, Q. Huang, Q. Bai, X. Yang, R. He, Y. Hao, H. Wang, T. Zhao, et al. 2015. The transcription factor TCF-1 initiates the differentiation of T_{FH} cells during acute viral infection. *Nat. Immunol.* 16:991–999. http://dx.doi.org/10.1038/ni.3229

Zaph, C., J. Uzonna, S.M. Beverley, and P. Scott. 2004. Central memory T cells mediate long-term immunity to *Leishmania major* in the absence of persistent parasites. *Nat. Med.* 10:1104–1110. http://dx.doi.org/10.1038/nm1108

Zhao, D.M., S. Yu, X. Zhou, J.S. Haring, W. Held, V.P. Badovinac, J.T. Harty, and H.H. Xue. 2010. Constitutive activation of Wnt signaling favors generation of memory CD8 T cells. *J. Immunol.* 184:1191–1199. http://dx.doi.org/10.4049/jimmunol.0901199

Zhou, X., S. Yu, D.M. Zhao, J.T. Harty, V.P. Badovinac, and H.H. Xue. 2010. Differentiation and persistence of memory $CD8^+$ T cells depend on T cell factor 1. *Immunity.* 33:229–240. http://dx.doi.org/10.1016/j.immuni.2010.08.002

Zhu, J., H. Yamane, and W.E. Paul. 2010. Differentiation of effector CD4 T cell populations. *Annu. Rev. Immunol.* 28:445–489. http://dx.doi.org/10.1146/annurev-immunol-030409-101212